SUPPLEMENTARY MATERIALS AND METHODS

In situ hybridization, Immunostaining, X-Gal staining and histology

In situ hybridization analysis of gene expression was performed using a protocol and digoxigenin-UTP cRNA probes that were previously described (Tam and Steiner, 1999; Hukriede et al., 2003; Fossat et al., 2007; Lewis et al., 2007; Fossat et al., 2011). Riboprobes for *Pcdh7 and Pcdh19* were synthesized with T7 polymerase using fragments amplified by PCR from cDNA of mouse embryoid bodies with the following primers: *Pcdh7*: 5'-CCCACTCACCCAGGATATA and 5'-ATCGTAATACGACTCACTATAGGGGTACTCGGAGCAGTGATCT; *Pcdh19*: 5'-CCACCAAGCCTTCTATATCT and 5'-ATCGTAATACGACTCACTATAGGGCACAACTGAATTTGCCTCTG.

Wholemount immunostaining adapted from (Burtscher and Lickert, 2009) was performed using primary antibodies against FOXA2 (1:1000; SC-6554; Santa Cruz Biotechnology) and E-Cadherin (1:300; 13-1900; Invitrogen). Embryo were also stained with DAPI (1:1000) and imaged (in separate channels) with a Leica SP5 confocal microscope.

X-Gal staining was performed as previously described (Lewis et al., 2007; Fossat et al., 2011). For histology, stained embryos were embedded in paraffin wax, sectioned and counter-stained with nuclear fast-red (Tam and Steiner, 1999; Lewis et al., 2007).

At least 3 specimens of each genotype were analysed for each staining.

Molecular cloning

The following mouse coding sequences were amplified by PCR from E7.5 embryos cDNA using the primers described below and cloned between the SalI and NotI sites of the pCMV-SPORT6 plasmid (Invitrogen) (*Ldb1*, *Ssbp3*) or between the SalI and XbaI sites of a pCMV-SPORT6 plasmid containing a HA tag coding sequence (primers 5'-CTAGATACCCATACGACGTTCCAGACTACGCTTAGC and 5'-TCGAGCTAAGCGTAGTCTGGAACGTCGTATGGGTAT cloned between the XbaI and XhoI sites) (*Lhx1* and

Lhx1Δ): (i) *Ldb1*: 5'-GATCGTCGACACCATGCTGGATCGGGATGTGG and 5'-GATCGCGGCCGCTACTTAT CGTCGTCATCCTTGTAATCCTGGGAAGCCTGTGACGTG; (ii) *Ssbp3*: 5'-GATCGTCGACACCATGTTTGCCAAA GGCAAAGG and 5'-GATCGCGGCCGCTACGTAGAATCGAGACCGAGGAGAGGGTTAGGGATAGGCTTACCC ACGCTCATCGTCATGCTC; (iii) *Lhx1*: 5'-GATCGTCGACACCATGGTGCACTGTGCGGGC and 5'-GATCTCTAG ACCACACGGCTGCCTCGTT; (iv) *Lhx1Δ* (Last ~500 bp of mouse *Lhx1* coding sequences that do not contain the DNA and the protein binding domains): 5'-GATCGTCGACACCATGAAACAGCTAAGCGCG CTAG and 5'-GATCTCTAGACCACACGGCTGCCTCGTT.

Vectors for luciferase assay: Genomic regions were amplified by PCR from mouse genomic DNA with primers described below and cloned into the XhoI site or between the NheI and the KpnI sites of the pGL3-promoter plasmid (Promega): (i) *Pcdh7* -0.2R: 5'-ATCGGGTACCGCGGCTGAGAATCCAAACTT and 5'-ATCGGCTAGCTCCTGCTTCTTCCGAAAGTT; (ii) *Pcdh7* +8.5R: 5'-ATCGCTCGAGGCACTAGTTAGTGGGA GAAA and 5'-ATCGCTCGAGACACTCAACCACAATGCTGA; (iii) Wild type or (iv) mutated dH1: 5'-ATCGCTCGAGCGAGGTTTGATTTGGGATCA and 5'-ATCGCTCGAGCACATGAGATCAAAGTGGCT. In the case of mutated dH1 where LHX1 binding site YTAATNN (Mochizuki et al., 2000; Sudou et al., 2012; Yasuoka et al., 2014) is mutated into YGCGCNN, fragment was amplified from two PCR products pooled and previously amplified with primers set 5'-ATCGCTCGAGCGAGGTTTGATTTGGGATCA and 5'-CTTTCTCGCGCGTGTTTCATATCGCTGAGCA and primers set 5'-TGAAACACGCGCGAGAAAGCCGGGAGC TAAG and 5'-ATCGCTCGAGCACATGAGATCAAAGTGGCT.

The sequence of the cloned fragments was verified by Sanger sequencing.

Cell transfection assays for RT-PCR and ChIP-PCR

Embryonal carcinoma P19 cells (in 10-cm dish) were transfected using Fugene 6 (Roche) with: (i) p*GFP* (pNF-5; (Fossat et al., 2014)) (1 µg) + mock plasmid (9 µg), (ii) p*GFP* (1 µg) + p*Lhx1-HA* (3 µg) + mock plasmid (6 µg), (iii) p*GFP* (1 µg) + p*Ldb1* (3 µg) + p*Ssbp3* (3 µg) + mock plasmid (3 µg), (iv) p*GFP* (1 µg) + p*Lhx1-HA* (3 µg) + p*Ldb1* (3 µg) + p*Ssbp3* (3 µg) or (v) p*GFP* (1 µg) + p*Lhx1Δ-HA* (3 µg) +

p*Ldb1* (3 µg) + p*Ssbp3* (3 µg). The mock plasmid is a pCMV-SPORT6 expressing a non-functional form of RBM47 that does not have any activity on head formation (Fossat et al., 2014). 24 h after transfection, GFP-expressing cells were sorted by flow cytometry and snap-frozen for storage until further analysis. Samples for ChIP-PCR analysis were treated with paraformaldehyde (for cross-linking) prior to storage.

Luciferase assay

Embryonal carcinoma P19 cells (in 1.5 cm well) were transfected using Fugene 6 (Roche) with pGL3-promoter only or pGL3-promoter containing either *Pcdh7* -0.2R, *Pcdh7* +8.5R, *Dkk1* dH1 or *Dkk1* mutated dH1 (0.25 µg) and (i) mock plasmid (0.75 µg), (ii) mock plasmid (0.50 µg) + p*Lhx1-HA* (0.25 µg), (iii) mock plasmid (0.50 µg) + p*Lhx1Δ-HA* (0.25 µg), (iv) mock plasmid (0.25 µg) + p*Ldb1* (0.25 µg) + p*Ssbp3* (0.25 µg) or (v) p*Ldb1* (0.25 µg) + p*Ssbp3* (0.25 µg) + p*Lhx1-HA* (0.25 µg). Cells were co-transfected with pRL renilla luciferase reporter vector (25 ng; Promega). Cells were collected 24 h after transfection, and luciferase assay was performed as described before (Ip et al., 2014) on three independent samples from each transfection experiment. Firefly luciferase activity was normalised against renilla luciferase activity.

RNA isolation and RT-qPCR

For the *Lhx1*-epiCKO study, three independent pools of five anterior fragments of mutant and control E7.75 embryos were analysed independently. For the *Lhx1*-ameCKO and the *Lhx1;Dkk1* study, anterior fragments of the E7.75 embryos (three or five per genotype) were analysed independently. For cell experiments, each replicate of flow-sorted GFP-expressing cells was analysed independently. Total RNA was extracted using the RNeasy Micro Kit (Qiagen). cDNAs were synthesized from 5-10 ng (individual embryos), 30-40 ng (pooled embryo fragments) or 100 ng (GFP cells) of total RNA using the Superscript III First Strand System (Invitrogen). Quantitative PCR was

performed in technical triplicate and normalised against *β-Actin* using protocol and primers described before (Fossat et al., 2011) or listed in Supplementary **Table S6A**.

ChIP-PCR analysis

Cells were cross-linked with 37% formaldehyde and sonicated to generate genomic DNA fragments of 200 to 1000 bp sizes. 20 μl of the fragmented chromatin was collected for the input. 50 μl (about one third of the chromatin obtained from 250000 cells) was incubated with rabbit polyclonal HA antibody (Santa Cruz, sc-805) overnight at 4°C with constant rotation. Cross-linking was reversed with protease K treatment (10 μg/μL) at 62°C overnight. Immuno-precipitated chromatin and input DNA were extracted in 20 μl water using phenol-chloroform purification protocol. PCR reaction was performed on 1 μl of DNA sample using Biomix Red (Bioline) Taq polymerase. Conditions were the same for all the PCRs: 94°C for 30 seconds, 60°C for 30 seconds, 72°C for 30 seconds for 35 cycles.

SUPPLEMENTARY FIGURES

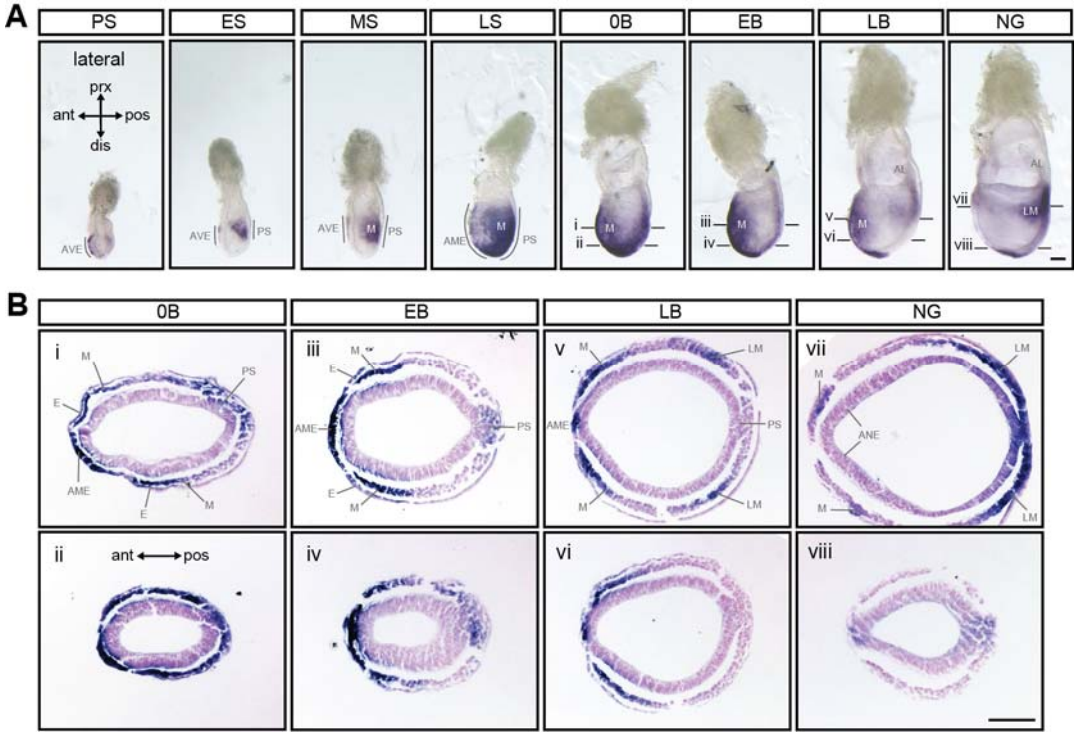

Figure S1. *Lhx1* expression pattern. (**A**) *Lhx1* whole mount in situ hybridization of wild type embryos at pre-streak (PS), early-streak (ES), mid-streak (MS), late-streak (LS), no-bud (OB), early-bud (EB), late-bud (LB) and neural-groove (NG) stages. (**B**) Histology of no-bud (OB), early-bud (EB), late-bud (LB) and neural-groove (NG) embryos shown part A. Plane of sectioning is indicated in A. AL, allantois; AME, anterior mesendoderm; ANE, anterior neurectoderm; ant, anterior; AVE, anterior visceral endoderm; dis, distal; E, endoderm; LM, lateral mesoderm; M, mesoderm; pos, posterior; prx, proximal; PS, primitive streak. Scale bars: 100 µm.

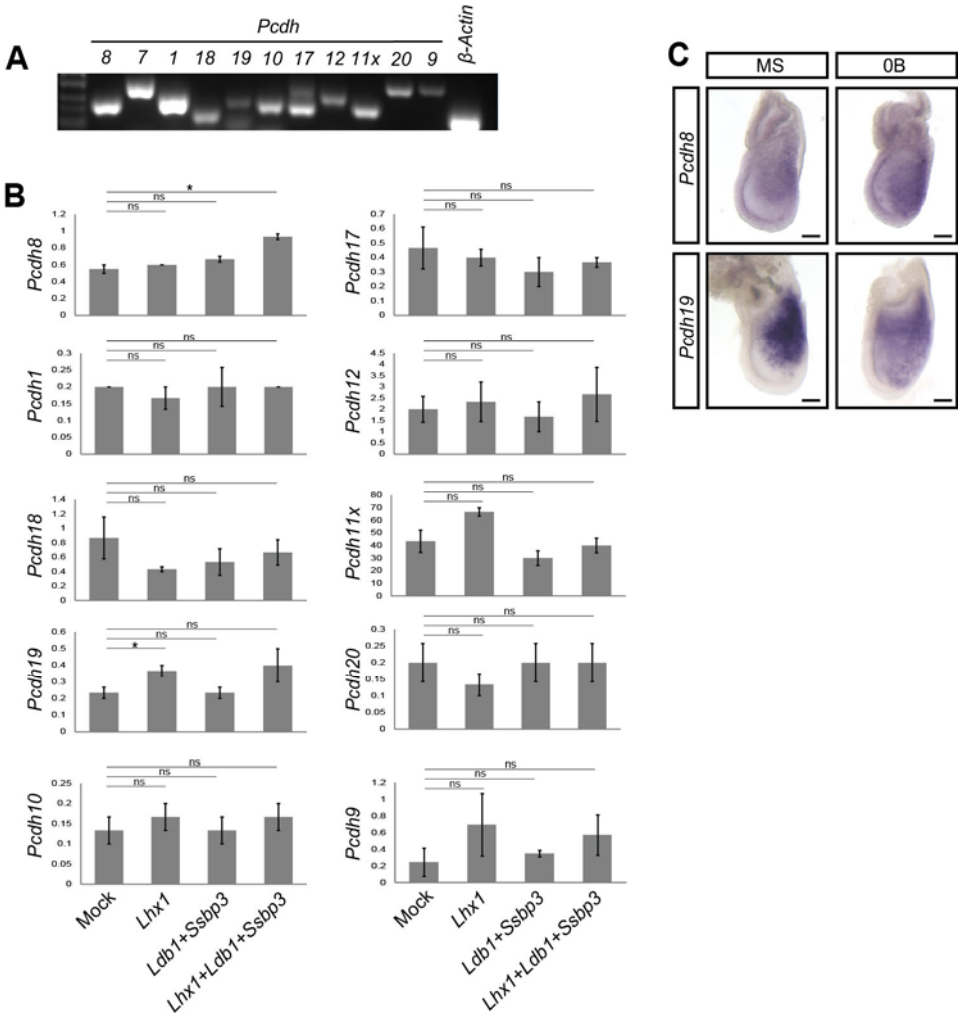

Figure S2. Expression of the *Pcdh* genes. (**A**) Expression of *Pcdh* gene family members (*Pcdh-1*, *-7*, *-8*, *-9*, *-10*, *-11x*, *-12*, *-17*, *-18*, *-19* and -20) relative to *β-Actin* in E7.75 mouse embryo analysed by RT-PCR. (**B**) Expression of *Pcdh* genes (relative to *β-Actin*) analyzed by RT-qPCR in P19 cells transfected with different combinations of vectors expressing a mock protein, *Lhx1, Ldb1* and/or *Ssbp3*. Data represent the mean ± standard errors of *N* = 3 independent experiments for each condition of transfection. *P*-value (*) < 0.05 and not significant (ns) by t-test. (**C**) Expression of *Pcdh8* and *Pcdh19* in the mesoderm but not in the anterior mesendoderm of the mid-streak (MS) and no-bud (0B) stage embryo. Lateral view of specimens with anterior to the left. Scale bars: 100 µm.

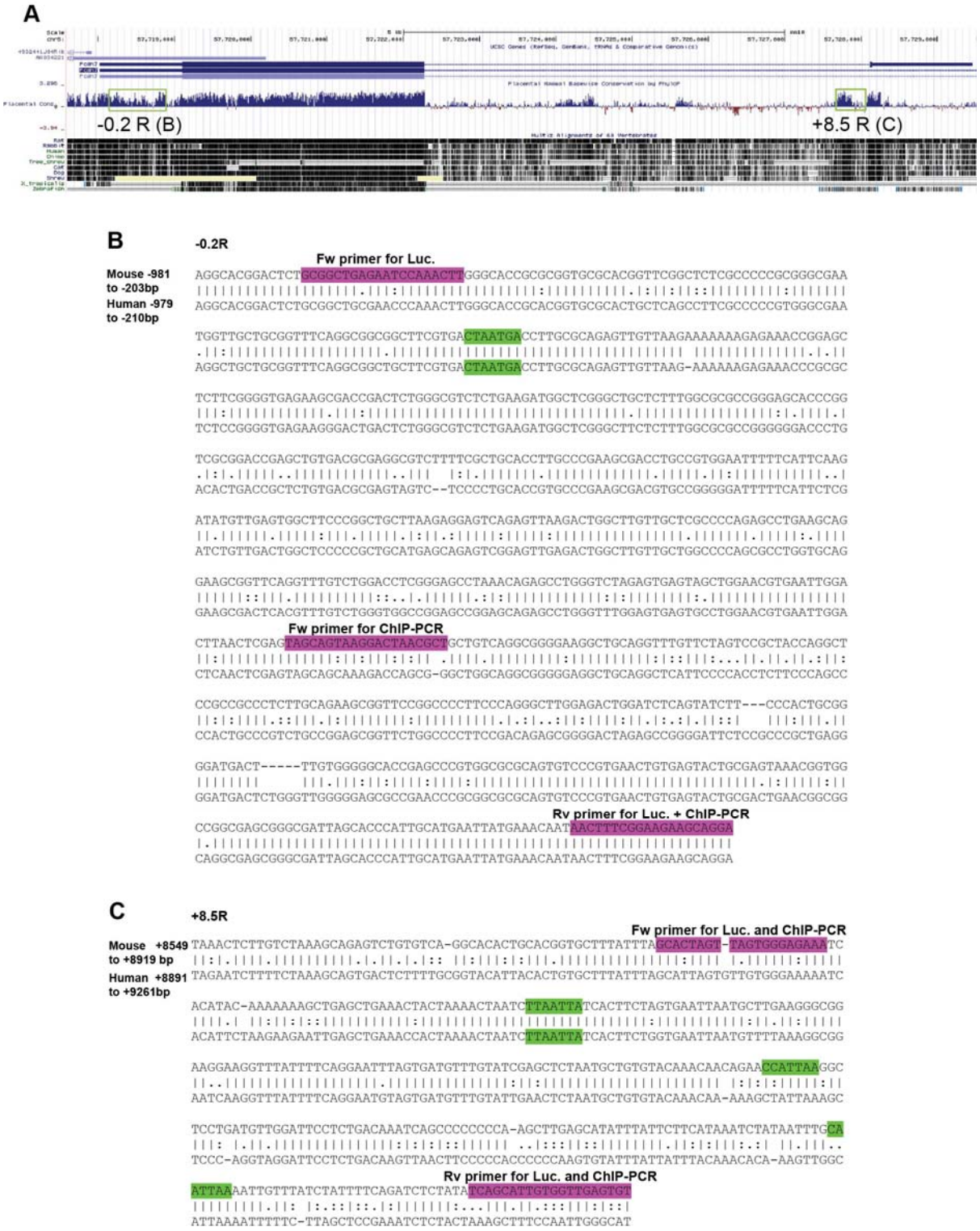

Figure S3. Mouse *Pcdh7* -0.2R and +8.5R regions. (**A**) Genomic information of the *Pcdh7* locus in sense orientation (UCSC genomic browser). Thick blue boxes indicate coding sequences and thin blue boxes indicate untranslated regions. Placental mammal base-wise conservation (Placental Cons)

histogram shows the result of multiple sequence alignment for 60 vertebrate species. The conservation score was measured by phyloP. The blue bar indicates positive score in which the regions are conserved, whereas regions with negative score in red indicate are not conserved. Gray scale density plot display pairwise alignments for each species (Rat, Rabbit, Human, Chimp, Dog, Tree Shrew, Cat, Dog, X tropicalis, Zebrafish). Gray scales with darker values indicate higher level of overall conservation scored by phastCons. The green box delineates the conserved genomic location covering the -0.2R and the +8.5R regions. (**B**) Basewise sequence alignment of the mouse (-981 to -203 bp upstream of START codon) and the human (-979 to -210bp upstream of START codon) *Pcdh7* -0.2R region. (**C**) Basewise sequence alignment of the mouse (+8549 to +8919 bp downstream of START codon) and the human (+8891 to +9261bp downstream of START codon) *Pcdh7* +8.5R region. Sequences of the primers used for ChIP-qPCR and luciferase (Luc.) assay are highlighted in purple. Fw, forward primer; Rv, reverse primer. Sequences highlighted in green are LHX1 recognition motifs.

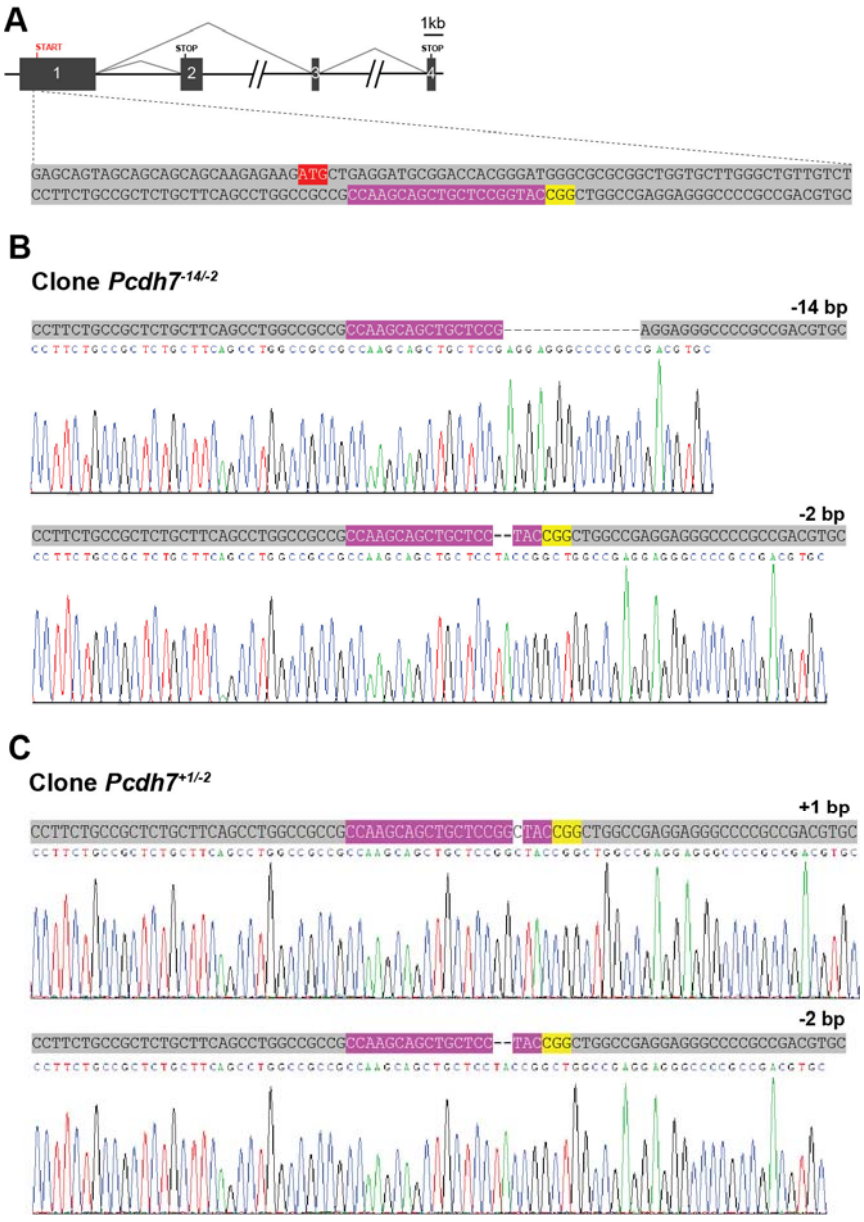

Figure S4. Mutant *Pcdh7* alleles generated by CRISPR-Cas9 editing. (**A**) Genome structure of the *Pcdh7* locus. Exons (grey boxes), splicing pattern (grey lines), START codon, STOP codon and the scale are indicated. Between dashed lines is a detailed view of the region downstream the START codon (ATG; highlighted in red) showing the sequence recognised by the sgRNA (highlighted in pink) used for experiment and the immediately adjacent PAM sequence (highlighted in yellow). (**B, C**) Mutant *Pcdh7* alleles of two independent ES cells clones obtained and used for the chimera experiments: (B) Clone $Pcdh7^{-14/-2}$: allele #1, 14 bp deletion; allele #2, 2 bp deletion, and (C) clone $Pcdh7^{+1/-2}$: allele #1, 1 bp insertion; allele #2, 2 bp deletion. Sanger sequencing chromatograms are

shown for each allele. The clones have been selected for the chimera experiments based on the fact that they have bi-allelic frame shift mutations of the open reading frame of the coding sequence of *Pcdh7*.

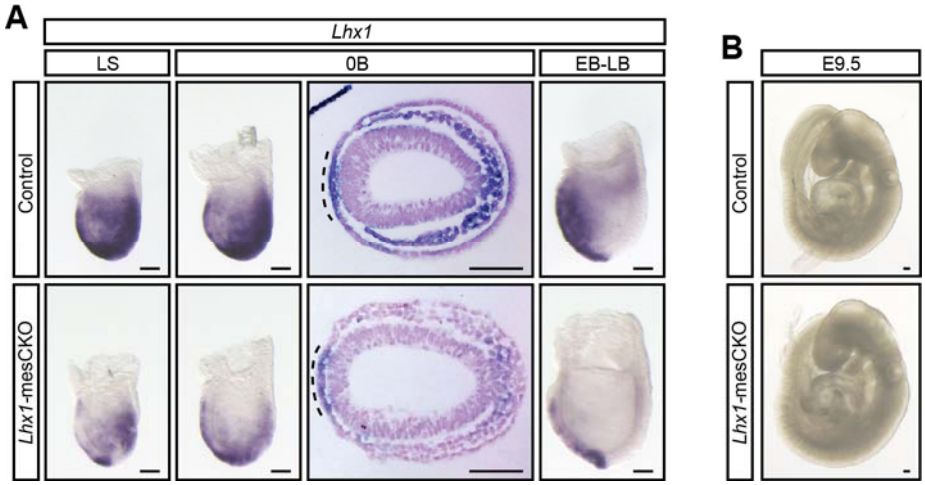

Figure S5. Conditional deletion of *Lhx1* in the mesoderm. (**A**) Detection of *Lhx1* RNA by whole mount in situ hybridization in late-streak (LS), no-bud (0B), early- to late-bud (EB-LB) control and *Lhx1*$^{-/flox}$;*Mesp1*^{Cre} (*Lhx1*-mesCKO) embryos. Transverse sections of 0B-stage *Lhx1*-mesCKO embryo shows the loss of *Lhx1* expression in the mesoderm, but expression was retained in the anterior mesendoderm (dashed line) and the nascent mesenchyme in the primitive streak. (**B**) E9.5 control and *Lhx1*-mesCKO embryos showing similar morphology. Lateral view of whole-mount specimens and sections with anterior side to the left. The cross between *Lhx1*$^{flox/flox}$ and *Lhx1*$^{+/-}$;*Mesp1*$^{+/Cre}$ mice generated embryos of four genotypes, which were present in a ratio consistent to the Mendelian distribution (*N* = 21, 3 litters: *Lhx1*$^{+/flox}$;*Mesp1*$^{+/+}$: 33%, *Lhx1*$^{+/flox}$;*Mesp1*$^{+/Cre}$: 24%, *Lhx1*$^{flox/-}$;*Mesp1*$^{+/+}$: 14% and *Lhx1*$^{flox/-}$;*Mesp1*$^{+/Cre}$: 29%). Scale bars: 100 µm.

A

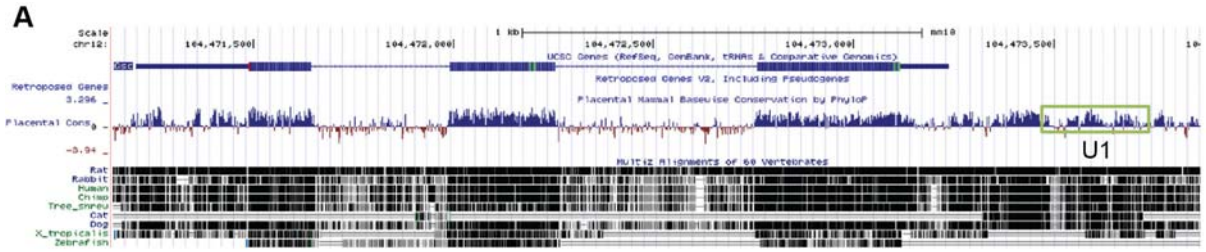

U1

Fw primer

Mouse -618 to -363bp AGAGGTCGG-CGG-CGGAGTTGTTAACGGCGGCAGGACAATAGTATTAATAAGATTAACCTGGGCAATTAGGCCGCCCGC

Human -560 to -331bp AGAGCTCGGGCGGAGGGAGTTGTTAACTGCGGCGGCACAAAGGAATTAATGAGATTAACCAAGGCAATTAGGC----CGC

CCAGCAAGGCCG---GGGCCGCGCCGGGGCTGCCGAATGGAAAAGATTAGGTTAATTTCATTAATTCTCAATCCACAATC

CCGCCCAGCTCGGCCGGCCCGCGGCCCGGCTGCCGAATGGAAAAGATTAGGTTAATTTCATTAATTCGCAATCCACAATC

T-TTTTCAGGCCCTGTGGCCCCCCTCCTCTTGGCATCTCTCCCCCTCCCCTGCAAGCGCCCCCCGCCCACCCCCACCTCC

TCTTTTCAGGCCTTGTAA----------CCCCCTCCCCT--TGGCACCTCTCCCCCTCCCCC-CAACC

Rv primer

CCATTCCACACCACCCAAAGG

CTCTTC--CCCCACCC-AAAG

B

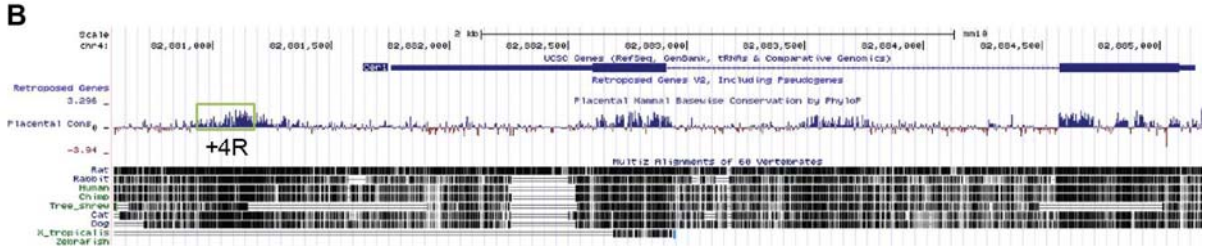

+4R

Fw primer

Mouse +3912 to +4155bp AGGATAAAATTGTTAAGCATTAATGATATCCCAGCTGGTCAATATATTTTGGTGCCAAAAGCTATTGAGCATCTGTCTAG

Human +4270 to +4513bp AGGATAAAATTGTTAAGCATTAATGATATCTCAGCTGGTCAATATATTTTGGTGCCAAAAGCTATCAAACAGCTGTCATG

TGTGCAACTGCCTAACCCTGATTATGTAAACCCATCTCTGCCAATTGGGGTCCCCTTCTCCTCCTTACATCTTCACAAAT

ATTGCAATCGCCTAACCCTGATTATGAAAACCTATCTCTGCCAATTGGACTGTCCTTCTCCTCCTTACATGCTTGTAAAT

Rv primer

CCCTTTTATCTATACTTGCAAATAGGCCCTCAAGCCCAAGCTCCAGACAATCATTAGTTTTATTCAAACTTCTGGCTTGC

CCGTTTCATCCATCCTTGCAAATAGACTCTCAAGCCCAAACCCCAAACAATGATCTGTTTTATTCAAATTTTGGTCTGCG

TCT

CTT

C

Figure S6. Mouse *Gsc* U1, *Cer1* +4R and *Dkk1* H1 regions. (**A**) Top: Genomic information of the mouse *Gsc* locus in antisense orientation (UCSC genomic browser). The green box delineates the conserved genomic location covering the U1 region. Bottom: Base-wise sequence alignment of the mouse (-618 to -363 bp upstream of START codon) and the human (-560 to -331bp upstream of START codon) U1 region. (**B**) Top: Genomic information of the mouse *Cer1* locus in antisense orientation (UCSC genomic browser). The green box delineates the conserved genomic location covering the +4R region. Bottom: Base-wise sequence alignment of the mouse (+3912 to +4155 bp downstream of START codon) and the human (+4270 to +4513bp downstream of START codon) +4R

region. (**C**) Top: Genomic information of the mouse *Dkk1* locus in antisense orientation (UCSC genomic browser). The green box delineates the conserved genomic location covering the H1 region. Bottom: Base-wise sequence alignment of the mouse (-1237 to -518 bp upstream of START codon) and the human (-1204 to -512bp upstream of START codon) H1 region {Kimura-Yoshida, 2005 #281}.Thick blue boxes indicate coding sequences and narrow blue boxes indicate untranslated regions. Placental mammal basewise conservation (Placental Cons) histogram shows the result of multiple sequence alignment for 60 vertebrate species. The conservation score was determined by phyloP. The blue bar indicates positive score for the conserved regions, whereas unconserved regions are marked with negative score in red. Gray scale density plot displays pairwise alignments for each species (Rat, Rabbit, Human, Chimp, Dog, Tree Shrew, Cat, Dog, X tropicalis, Zebrafish). Gray scales with darker values indicate higher level of overall conservation scored by phastCons. Sequences of the primers used for ChIP-PCR and luciferase assay are highlighted in purple. Fw, forward primer; Rv, reverse primer. Sequences highlighted in green are LHX1 recognition motifs.

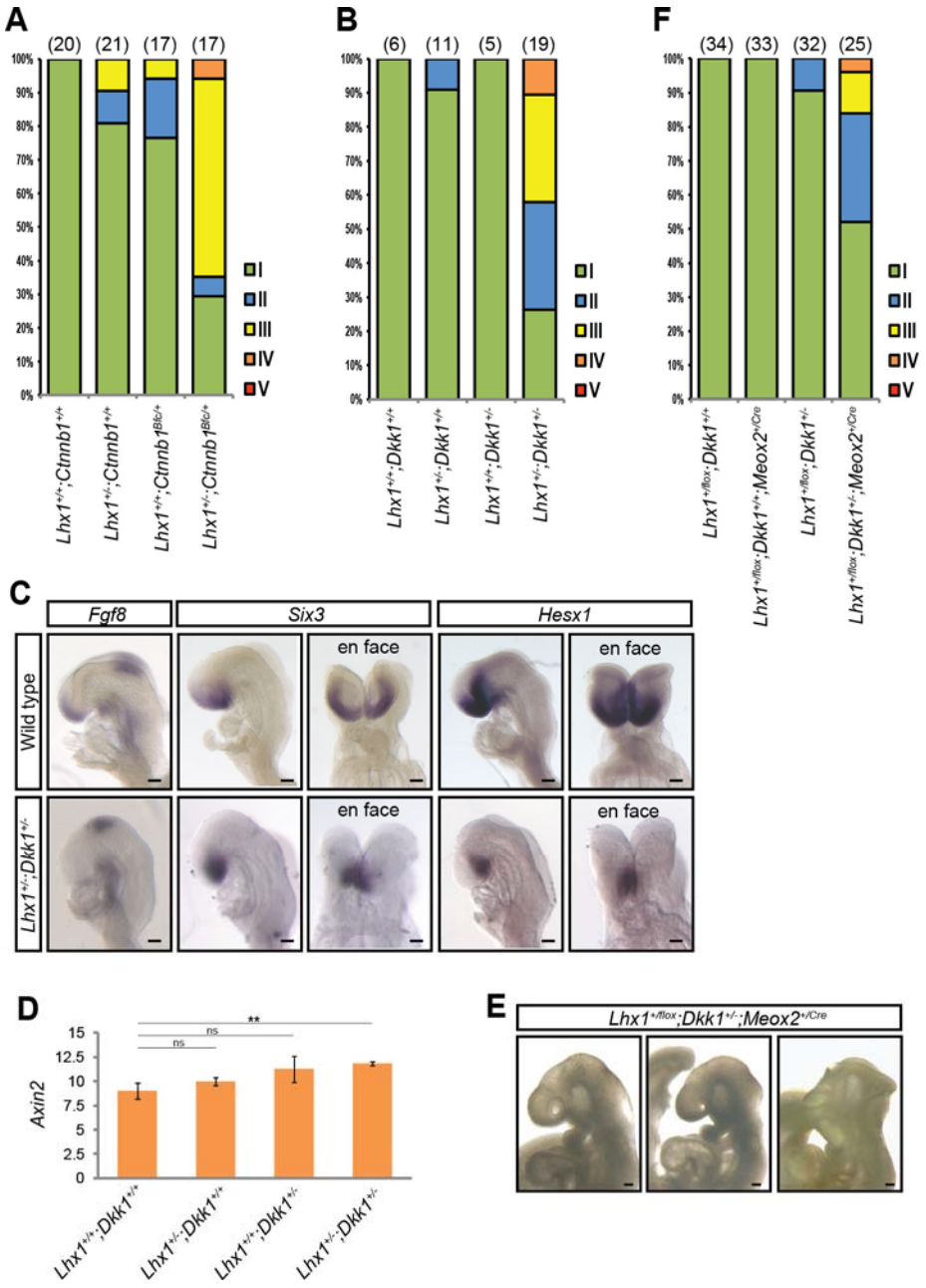

Figure S7. Genetic interaction of *Lhx1* activity and WNT signalling. (**A, B, F**) Histograms representing the distribution of the embryos of the different genotypes (X-axis) to the five head phenotype categories (colour-coded on the right). The categories are based on the size of the fore- and midbrain: [I] Normal size, [II] slight reduction (≤25%), [III] strong reduction (26-75% reduction), [IV] tissue remnant (>75% reduction), [V] tissues absent. The height of the bar indicates the percentage of embryos of each phenotype category. The number of embryos scored for each genotype is given

in parentheses. (**C**) Absence of *Fgf8* expression and reduced domains of expression of *Six3* and *Hesx1* in the anterior brain parts of E8.5 *Lhx1*$^{+/-}$*;Dkk1*$^{+/-}$ embryos (bottom panels), compared with the expression of the same markers in the wild type embryos (top panels). (**D**) RT-qPCR analysis of the expression of the WNT target *Axin2* (relative to *β-Actin*) in the anterior germ layer tissues of E7.75 early-bud to head-fold stage *Lhx1*$^{+/-}$*;Dkk1*$^{+/-}$, *Lhx1*$^{+/-}$, *Dkk1*$^{+/-}$ and wild-type embryos. Data represent the mean ± standard errors of *N* = 5 embryos analysed for each genotype, except *N* = 3 for *Lhx1*$^{+/-}$ embryos. *P*-value < 0.01 (**), no significant difference (ns) by t-test. (**E**) Truncated head phenotype of *Lhx1*$^{+/flox}$*;Dkk1*$^{+/-}$*;Meox2*$^{+/Cre}$ E9.5 mutant embryos. Lateral view of specimens with anterior side to the left, except for *en face* views. Scale bars: 100 µm.

Table S1. Phenotypic analysis of *Lhx1*-epiCKO mutant embryos.

Frequency of abnormal head phenotype for E8.5-E10.5 embryos generated from crosses between *Lhx1*$^{flox/flox}$ and *Lhx1*$^{+/-}$;*Meox2*$^{+/Cre}$ mice.

Number of embryos (number showing head abnormality)				
Genotype	*Lhx1*$^{+/flox}$	*Lhx1*$^{-/flox}$	*Lhx1*$^{+/flox}$;*Meox2*$^{+/Cre}$	*Lhx1*$^{-/flox}$;*Meox2*$^{+/Cre}$
	41 (0)	25 (0)	32 (1)	38 (38)
% with head defects	0%	0%	3.1%	100%

All the *Lhx1*$^{-/flox}$;*Meox2*$^{+/Cre}$ mutant embryos displayed category V head defects.

Table S2. Phenotypic analysis of *Lhx1*-ameCKO mutant embryos.

A. Frequency of abnormal head phenotype for E9.5 embryos generated from crosses between *Lhx1*$^{flox/flox}$ and *Lhx1*$^{+/-}$;*Foxa2*$^{+/mcm}$ or *Lhx1*$^{+/-}$;*Foxa2*$^{mcm/mcm}$ mice injected with oil only (Mock) or tamoxifen (Tam).

Number of embryos (number showing head abnormality)								
Genotype	*Lhx1*$^{+/flox}$;*Foxa2*$^{+/+}$		*Lhx1*$^{+/flox}$;*Foxa2*$^{+/mcm}$		*Lhx1*$^{flox/-}$;*Foxa2*$^{+/+}$		*Lhx1*$^{flox/-}$;*Foxa2*$^{+/mcm}$	
Injection	Mock	Tam	Mock	Tam	Mock	Tam	Mock	Tam
	3 (0)	3 (0)	13 (4)	10 (2)	3 (0)	4 (1)	14 (2)	10 (9)
% with head defects	0%	0%	31%	20%	0%	25%	14%	90%

B. Categories of the head phenotype of *Lhx1*$^{flox/-}$;*Foxa2*$^{+/mcm}$ embryos.

	Number of embryos per head phenotype category					**Number of embryo (%) with head defect**
Phenotype category	I	II	III	IV	V	
Genotype						
Lhx1$^{flox/-}$;*Foxa2*$^{+/mcm}$ Mock	12	1	1	0	0	2 (14%)
Lhx1$^{flox/-}$;*Foxa2*$^{+/mcm}$ Tam	1	3	3	1	2	9 (90%)

$P<0.01$ by χ^2 test for the distribution of the embryos across the phenotype categories between the two treatment groups.
Affected embryos of the other genotypes (see part A) displayed category II phenotype.

Table S3. Phenotypic analysis for genetic interaction of *Lhx1* and *Ctnnb1*.

A. Frequency of abnormal head phenotype for E9.5 embryos generated from crosses between *Lhx1*$^{+/-}$ and *Ctnnb1*$^{Bfc/+}$ mice.

Number of embryos (number showing head abnormality)				
Genotype	*Lhx1*$^{+/+}$;*Ctnnb1*$^{+/+}$	*Lhx1*$^{+/-}$;*Ctnnb1*$^{+/+}$	*Lhx1*$^{+/+}$;*Ctnnb1*$^{Bfc/+}$	*Lhx1*$^{+/-}$;*Ctnnb1*$^{Bfc/+}$
	20 (0)	21 (4)	17 (4)	17 (12)
% with head defects	0%	19%	24%	71%

B. Categories of head phenotype.

	Number of embryos per head phenotype category					**Number of embryo (%) with head defect**
Phenotype category / **Genotype**	I	II	III	IV	V	
Lhx1$^{+/+}$;*Ctnnb1*$^{+/+}$	20	0	0	0	0	0 (0%)
Lhx1$^{+/-}$;*Ctnnb1*$^{+/+}$	17	2	2	0	0	4 (19%)*
Lhx1$^{+/+}$;*Ctnnb1*$^{Bfc/+}$	13	3	1	0	0	4 (24%)ǂ
Lhx1$^{+/-}$;*Ctnnb1*$^{Bfc/+}$	5	1	10	1	0	12 (71%)*ǂ

*P<0.01 by χ^2-test for difference in the distribution of the embryos across the phenotype categories between *Lhx1*$^{+/-}$;*Ctnnb1*$^{Bfc/+}$ embryos and *Lhx1*$^{+/-}$;*Ctnnb1*$^{+/+}$ embryos.
ǂP<0.01 by χ^2-test for difference in the distribution of the embryos across the phenotype categories between *Lhx1*$^{+/-}$;*Ctnnb1*$^{Bfc/+}$ embryos and *Lhx1*$^{+/+}$;*Ctnnb1*$^{Bfc/+}$ embryos.

Table S4. Phenotypic analysis for genetic interaction of *Lhx1* and *Dkk1*.

A. Frequency of abnormal head phenotype for E8.5-E9.5 embryos generated from intercross of *Lhx1*$^{+/-}$;*Dkk1*$^{+/-}$ mice.

Number of embryos (number showing head abnormality)				
Genotype	*Lhx1*$^{+/+}$;*Dkk1*$^{+/+}$	*Lhx1*$^{+/-}$;*Dkk1*$^{+/+}$	*Lhx1*$^{+/+}$;*Dkk1*$^{+/-}$	*Lhx1*$^{+/-}$;*Dkk1*$^{+/-}$
	6(0)	11 (1)	5 (0)	19 (14)
% with head defects	0%	9%	0%	74%

All *Lhx1*$^{+/+}$; *Dkk1*$^{-/-}$, *Lhx1*$^{-/-}$; *Dkk1*$^{+/+}$, *Lhx1*$^{-/+}$; *Dkk1*$^{-/-}$, *Lhx1*$^{-/-}$; *Dkk1*$^{+/-}$ and *Lhx1*$^{-/-}$; *Dkk1*$^{-/-}$ embryos also generated in this cross displayed defect as *Lhx1* or *Dkk1* homozygous null embryos (data not shown).

B. Categories of head phenotype.

	Number of embryos per head phenotype category					**Number of embryo (%) with head defect**
Phenotype category	I	II	III	IV	V	
Genotype						
Lhx1$^{+/+}$;*Dkk1*$^{+/+}$	6	0	0	0	0	0 (0%)
Lhx1$^{+/-}$;*Dkk1*$^{+/+}$	10	1	0	0	0	1 (9%)*
Lhx1$^{+/+}$;*Dkk1*$^{+/-}$	5	0	0	0	0	0 (0%)ŧ
Lhx1$^{+/-}$;*Dkk1*$^{+/-}$	5	6	6	2	0	14 (74%)*ŧ

*P<0.01 by χ^2-test for difference in the distribution of the embryos across the phenotype categories between *Lhx1*$^{+/-}$;*Dkk1*$^{+/-}$ and *Lhx1*$^{+/-}$;*Dkk1*$^{+/+}$ embryos.
ŧP<0.05 by χ^2-test for difference in the distribution of the embryos across the phenotype categories between *Lhx1*$^{+/-}$;*Dkk1*$^{+/-}$ and *Lhx1*$^{+/+}$;*Dkk1*$^{+/-}$ embryos.

Table S5. Phenotypic analysis for genetic interaction of *Lhx1* and *Dkk1* in the epiblast.

A. Frequency of abnormal head phenotype for E8.5-E10.5 embryos generated from crosses between *Lhx1$^{flox/flox}$* and *Dkk1$^{+/-}$;Meox2$^{+/Cre}$* mice.

Number of embryos (number showing head abnormality)				
Genotype	*Lhx1$^{+/flox}$;Dkk1$^{+/+}$*	*Lhx1$^{+/flox}$;Dkk1$^{+/+}$;Meox2$^{+/Cre}$*	*Lhx1$^{+/flox}$;Dkk1$^{+/-}$*	*Lhx1$^{+/flox}$;Dkk1$^{+/-}$;Meox2$^{+/Cre}$*
	34 (0)	33 (0)	32 (3)	25 (12)
% with head defects	0%	0%	9.5%	48%

B. Categories of head phenotype.

	Number of embryos per head phenotype category					**Number of embryo (%) with head defect**
Phenotype category	I	II	III	IV	V	
Genotype						
Lhx1$^{+/flox}$;Dkk1$^{+/+}$	34	0	0	0	0	0 (0%)
Lhx1$^{+/flox}$;Dkk1$^{+/+}$;Meox2$^{+/Cre}$	33	0	0	0	0	0 (0%)*
Lhx1$^{+/flox}$;Dkk1$^{+/-}$	29	3	0	0	0	3 (9.5%)ŧ
Lhx1$^{+/flox}$;Dkk1$^{+/-}$;Meox2$^{+/Cre}$	13	8	3	1	0	12 (48%)*ŧ

*P<0.001 by χ^2-test for difference in the distribution of the embryos across the phenotype categories between *Lhx1$^{+/flox}$;Dkk1$^{+/-}$;Meox2$^{+/Cre}$* and *Lhx1$^{+/flox}$;Dkk1$^{+/+}$;Meox2$^{+/Cre}$* embryos.
ŧP<0.01 by χ^2-test for difference in the distribution of the embryos across the phenotype categories between *Lhx1$^{+/flox}$;Dkk1$^{+/-}$;Meox2$^{+/Cre}$* and *Lhx1$^{+/flox}$;Dkk1$^{+/-}$* embryos.

Table S6. Sequences of primers for RT-PCR and ChIP-PCR.

A. RT-PCR Primers.

Gene	Sense primer	Antisense primer
Pcdh1	5'-GCTTCGTGTCACTGTGCTT	5'-GTGTTTCGGTCTAGTCGCA
Pcdh7	5'-CCTGTACATAGAGGAGAACA	5'-AGCTACTACTGTCCTGACAT
Pcdh8	5'-TTCAATGACAGTGACTCGGA	5'-GAAGGTTGACATCTGGGCT
Pcdh9	5'-CAGGAAAGCTGCAGTGACA	5'-ACATCTCTGTAGCTTCAGCT
Pcdh9	5'-TTCAGATCACTTCAGTGCCT	5'-TCGAATGTGGAAACTGGTAG
Pcdh10	5'-CCAGGAAGCTGACATAGTAA	5'-AAGGGACAAAAGAAGGCATC
Pcdh11x	5'-ACTCGGCTATAAACTCTCGA	5'-TTGAACAATCAGTTGGGGCA
Pcdh12	5'-TCAATGGCAAAGTGTCTCCT	5'-TTATTTCCTCGGTGGTTTGG
Pcdh17	5'-CAGTGACCAAGACACTAACA	5'-ATCAGAATGACCAAGCACTC
Pcdh18	5'-ATTCAGTGACCTCTTCCTCA	5'-TTGCTTCTGTAGTCAGAGGA
Pcdh19	5'-CACTATGATCTTCGTGGCAA	5'-TGTCTTGCTCCTCACTATTG
Pcdh20	5'-CCAGTATGTGACCCTAAACA	5'-AACTGCGGAGCATTGTCATT
Hesx1	5'-AGCATTTTAGGACTGGACCA	5'-ATGAAGTCTCACTGGGAAGA
Cer1	5'-GCATCGGTTCATGTTCAGAA	5'-GAACTGCATTTGCCAAAGCA
Gsc	5'- TGGAGAACCTCTTCCAGGA	5'- AGGATCGCTTCTGTCGTCT
Lef1	5'-AACTGGCATCCCTCATCCA	5'-GCTACGACATTCGCTCTCA

B. ChIP-PCR primers.

Region	Sense primer	Antisense primer
Pcdh7 -0.2R	5'-TAGCAGTAAGGACTAACGCT	5'-TCCTGCTTCTTCCGAAAGTT
Pcdh7 +8.5R	5'-GCACTAGTTAGTGGGAGAAA	5'-ACACTCAACCACAATGCTGA
Dkk1 dH1	5'-CGAGGTTTGATTTGGGATCA	5'-CACATGAGATCAAAGTGGCT
Hesx1 dp	5'-CGTTCTGCTTAGGAGAGATA	5'-CCTTGTAGCTTTGCTGACTA
Gsc U1	5'-TTAACGGCGGCAGGACAAT	5'-CCTTTGGGTGGTGTGGAAT
Cer1 +4R	5'-TGATATCCCAGCTGGTCAAT	5'-AGAGCAAGCCAGAAGTTTGA
Non target	5'-TGTTCCCGGAAGTGGTTAAT	5'-CTCTTATTGGGTACTCCTGA

SUPPLEMENTARY REFERENCES

Fossat, N., Le Greneur, C., Beby, F., Vincent, S., Godement, P., Chatelain, G. and Lamonerie, T. (2007). A new GFP-tagged line reveals unexpected Otx2 protein localization in retinal photoreceptors. *BMC Dev Biol* **7**, 122.

Fossat, N., Tourle, K., Radziewic, T., Barratt, K., Liebhold, D., Studdert, J. B., Power, M., Jones, V., Loebel, D. A. and Tam, P. P. (2014). C to U RNA editing mediated by APOBEC1 requires RNA-binding protein RBM47. *EMBO Rep* **15**, 903-910.

Tam, P. P. and Steiner, K. A. (1999). Anterior patterning by synergistic activity of the early gastrula organizer and the anterior germ layer tissues of the mouse embryo. *Development* **126**, 5171-5179.